16TH EUROPEAN CONFERENCE ON EARTHQUAKE ENGINEERING THESSALONIKI 18 - 21 JUNE 2018

SHEAR WAVE VELOCITY VARIATIONS AT THE CORSSA (CENTRAL GREECE) VERTICAL ARRAY

Zafeiria ROUMELIOTI[1], Fabrice HOLLENDER[2], Philippe GUEGUEN[3]

ABSTRACT

We apply seismic interferometry by deconvolution to accelerometric data of the 178 m deep, 5-sensor vertical COrinth Rift Soft Soil Array (CORSSA), which is located at the southern coast of the Gulf of Corinth in central Greece. Our aim is to investigate orientation-related and temporal variations of shear wave velocities within the soil column and to seek indication for possible nonlinear response of the softer layers. We process the acceleration records of 709 seismic events, spanning the ranges 1.15-6.5 for the local magnitude and 1-281 km for the epicentral distance. We estimate shear-wave velocities at four depth intervals, i.e., between pairs of successive downhole sensors and examine their variations with respect to monthly precipitation data for the broader area, as well as to borehole-source azimuth. We conclude a seasonal variation of the inferred shear-wave velocities at shallow layers, which diminishes with depth and becomes untraceable at depths larger than 30 m. We also observe azimuthal dependence of the measured velocities, which varies with depth. The mean anisotropy over the entire soil column does not present sharp fast-shear and slow-shear directions, but rather ranges of azimuths of high and low shear-wave velocities, well separated by narrow azimuthal bands of sudden change in the measured values. Sudden reduction in the shear-wave velocity value is also inferred by the interferometry analysis of the strongest record in the dataset (peak ground acceleration above 90 cm/sec^2), suggesting the emergence of effects of nonlinear behavior of the soil at the examined site.

Keywords: Interferometry; Anisotropy; Nonlinear Response; Site Effects

1. INTRODUCTION

It is generally accepted that the realistic prediction of site effects and the nonlinear behavior of soil are key elements in seismic hazard assessment. One of the major difficulties in the study of the aforementioned elements is the definition of the reference ground motion. This difficulty can be overcome to a significant extent at sites being monitored by vertical arrays of accelerographs and/or velocimeters. The linear arrays provide the possibility to study the alterations of ground motion as the seismic waves propagate into the soil column with respect to record at the base, which is less affected by possible site effects. One of the tools that have been tentatively in use during the last decades in such studies is the seismic interferometry by deconvolution. The wide applicability of this method is due to its robustness and effectiveness in the extraction of shear wave velocity between pairs of successive sensors in a linear array (e.g., Sawazaki et al. 2009; Nakata and Snieder, 2011, 2012; Mehta et al. 2007; Chandra et al. 2015, Guéguen, 2015; Bonilla et al. 2017).
In the present work we examine acceleration data recorded at the Corinth Rift Soft Soil Array (CORRSA), a vertical array of accelerometers located in Aigio, a town at the southern shore of the Gulf of Corinth, in central Greece. Through the interferometry analysis between pairs of sensors of the vertical array, we aim to identify and, if possible, quantify variations in the velocity of shear seismic

[1] Department of Civil Engineering, Aristotle University of Thessaloniki, Thessaloniki, Greece, zroum@auth.gr
[2] CEA/DEN, 13108 Saint Paul Lez Durance, France // ISTerre, University Grenoble-Alpes / CNRS / IFSTTAR / IRD / USMB, France, fabrice.hollender@cea.fr
[3] ISTerre, University Grenoble-Alpes / CNRS / IFSTTAR / IRD / USMB, Grenoble, France, philippe.gueguen@univ-grenoble-alpes.fr

waves within the shallow soil formations at CORSSA. Among the different possible expressions of such variations, we concentrate our interest on seasonal, azimuthal and those caused by nonlinear behavior of the soil.

2. THE CORSSA SITE AND ARRAY

CORRSA is located in the port area of Aigio, a town lying on the south side of the Gulf of Corinth, in central Greece (Figure 1a). The 120° trending, 130-km long gulf comprises a young asymmetric rift, which is deforming with one of the highest rates in the Euro-Mediterranean region, under the approximately north-south (N-S) oriented back-arc extension of the Aegean microplate (e.g., Armijo et al. 1996; Jolivet et al. 2010; Reilinger et al. 2010). Most of the deformation in the area is taken up by normal faults of east-west to southeast-northwest orientation, among which is the closest to the CORSSA test site north-dipping Aigio fault (Figure 1; e.g., Koukouvelas and Doutsos, 1996; Koukouvelas, 1998; Palyvos et al. 2005).

The CORSSA downhole accelerometer array was installed in the frame of the European Union (EU) funded research project CORSEIS (EU reference number: EVG1-CT-1999-00002), the first in a series of projects that led to the development of the Corinth Rift Laboratory (CRL; http://crlab.eu/). The array consists of an 18-channel digitizer (Mt Whitney) equipped with 5 three-component broadband accelerometers: one sensor at the ground surface (Episensor, ES-T) and four sensors (FBA-23DH) installed in boreholes at depths of 14, 31, 57 and 178 m.

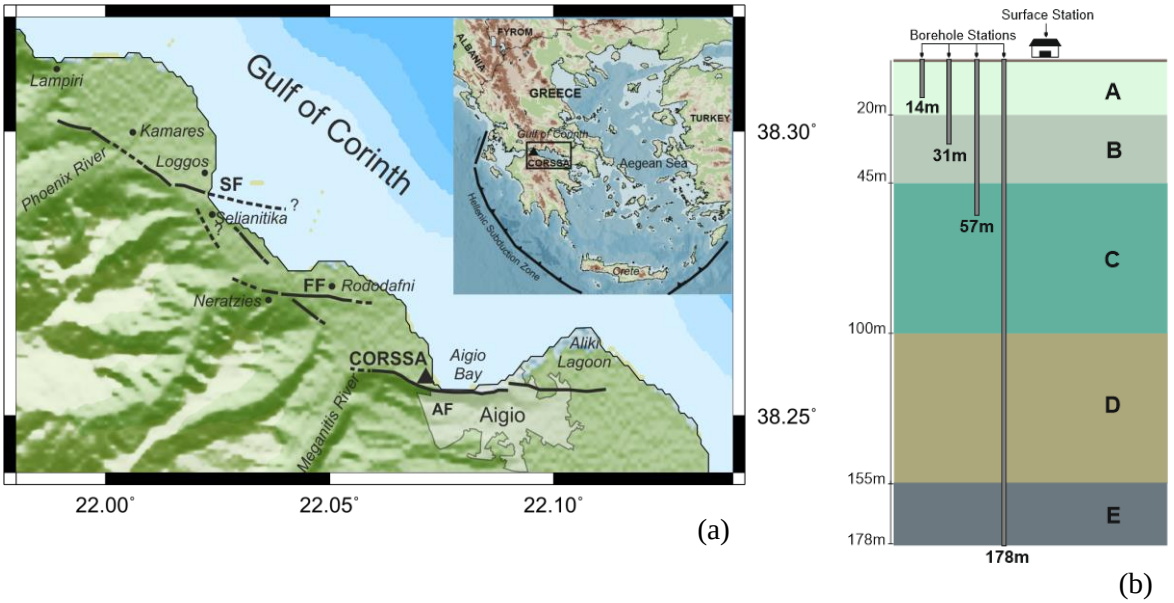

Figure 1. The CORSSA array; Left: Regional map showing the location of the downhole array. Fault lines (continuous=mapped, dashed=uncertain) along the coast of the broader Aigio area (from Koukouvelas and Doutsos, 1996, Palyvos et al., 2005 and references therein; AF: Aigio Fault, FF: Fassouleika Fault, SF: Selianitika Fault) are also shown. Onset map marks the location of the Gulf of Corinth (black frame). Right: layout of the sensors of the vertical array and gross geotechnical model (Apostolidis et al., 2006) for the CORSSA site. Description of formations A-E is given in Table 1.

Figure 1b includes a schematic presentation of the vertical array and the geotechnical model of the soil column at the CORSSA site, as proposed by Apostolidis et al. (2006). In the model of Apostolidis et al. (2006) sediments stiffness increases with depth and the deepest formation (E), a well-cemented conglomerate, comprises the geotechnical bedrock. The geological description of formations A-E, as well as their basic properties are listed in Table 1.

Table 1: Soil formation properties at CORSSA according to the model of Apostolidis et al. (2006): Geological description of the formations, formation thickness, number of counts in Standard Penetration Tests (N_{SPT}) and shear wave velocity, V_S. Formation codes are as in Figure 1b.

Formation Code	Geological Description	Thickness (m)	N_{SPT}	V_S (m/sec)
A	Soft marine deposits consisting of sandy silt, silt and clay	20	8-14	180
B	Soft sediments: clayey silt, sandy clay, silty clay, with few gravels	25	14-20	265
C	Hard deposits: clayey silt, sandy clay, silty clay, with few gravels	55	30-45	440
D	Very hard deposits: sandy gravels, sandy clay with few gravels	55	>80	540
E	Stiff conglomerate	-	-	1000

3. DATA

The CORSSA array was in operation for most of the time in the period from 2002 to 2012, with its data being collected and stored by the Seismological Laboratory of NKUA (National Kapodistrian University of Athens). Recently, CORSSA data were organized in a database, which became available to the scientific community through a dedicated web portal (http://www.corssa.gr/; Kassaras et al. 2016). This open source has been the basis of our starting dataset. Out of the 714 online available records, we selected the horizontal waveforms of 709, i.e., 1418 acceleration time histories in total, rejecting only a few corresponding to events at large distances, which had been triggered with a delay, thus missing the initial part of the earthquake ground motion. The processed dataset includes events of local magnitude, M_L, in the range 1.15-6.5 and distances from 1 to 281 km, which occurred from May 2002 to April 2012. The distribution of magnitudes and mean horizontal Peak Ground Acceleration (PGA) values with respect to epicentral distance, R, of the events is presented in Figure 2. Processed records are of weak ground motion (< 30 cm/sec^2), except those of the 08 June 2008, M_w6.4 earthquake (e.g., Gallovic et al. 2009; Ganas et al. 2009) at R = 58 km to the south-west (SW) of CORSSA, hereafter referred to as the "2008 SW Achaia earthquake".

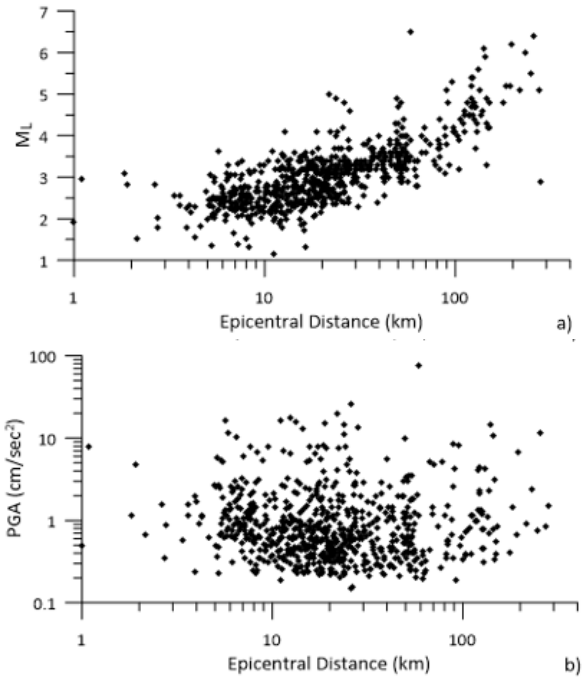

Figure 2. a) Local magnitude (M_L)-distance (R) and b) mean horizontal Peak Ground Acceleration (PGA)-distance distribution for the used set of accelerograms.

Accelerograms in the CORSSA database are available in homogenized form in terms of their units and orientation (E-W, N-S) and corrected to a zero-mean of their length and possible linear trends (Kassaras et al. 2016). We further processed the records by cutting the desired waveform parts and band-pass filtering. More specifically, to avoid introducing long low signal-to-noise parts of the waveforms in our analysis, we cut the recordings from their original zero point to the time corresponding to the 75% of the normalized Arias intensity, thus keeping the most energetic phases (Abrahamson, 2007). Then, prior to filtering, we tapered the waveforms with a half-cosine window and zero padded them to a total duration of 50 sec to ensure the effective application of the filter (Boore and Bommer, 2005). The applied filter was a fourth-order Butterworth band-pass with corners at 0.5 and 20 Hz.

3. SHEAR-WAVE VELOCITY ASSESSMENT

Seismic interferometry by deconvolution consists in removing the source signal by means of spectra division of the wave fields at two receivers. In this way, it is possible to obtain the impulse response of the propagation medium in the between the receivers region. In vertical arrays, the result of the interferometry by deconvolution is the causal and acausal propagation of waves within the system, i.e., an upward and a downward propagating pulse. The time difference in the arrival of the pulse at two receivers is related to the wave propagation velocity in the in-between medium.
The response between two receivers, *j* and *i*, is computed (e.g., Chandra et al. 2015, Guéguen 2016) as:

$$D_{j-i}(t) = FT^{-1}\left\{\frac{A_i(\omega)}{max\left\{A_j(\omega),\ k\left(|A_j(\omega)|,\ \frac{A_j(\omega)}{|A_j(\omega)|}\right)_{max}\right\}}\right\} \quad (1)$$

where ω is the angular frequency, $A_j(\omega)$ the Fourier transform of the recording at the j^{th} receiver, $A_i(\omega)$ is the reference signal, i.e., Fourier transform of the recording at the i^{th} receiver, and k is the "water-level" parameter that is being introduced to stabilize the deconvolution at very low values of the denominator (Clayton and Wiggins, 1976). After $D_{j-i}(\omega)$ has been computed, its inverse Fourier transformation is performed to obtain the propagating pulse and measure its travel time from *j* to *i* receiver, $\Delta t_{j\text{-}i}$. Subsequently, $\Delta t_{j\text{-}i}$ and the distance between receivers *j* and *i*, $\Delta h_{j\text{-}i}$, are used to estimate the equivalent linear shear-wave velocity from:

$$V_S = \frac{\Delta h_{j-i}}{\Delta t_{j-i}} \quad (2)$$

In our applications we used k = 10% and resampled the inverse Fourier transform of $D_{j-i}(\omega)$ using a ten times smaller step to improve the accuracy in the selection of the pulse travel time. We used the top-most point of the up-going pulse to define the travel time at each receiver. In order for the time measurement to be regarded as reliable, we set the prerequisite of its amplitude being at least 1.5 times larger the amplitude of the second largest peak in the causal part of the wave propagation. It is reminded that the same filter has been applied to all waveforms (pass band is 0.5-20 Hz) prior deconvolution. Examples of results for two events, a small magnitude one, close to CORSSA site (M_L3.1, R=23 km) and a larger one (M_L4.4) at epicentral distance greater than 80 km, are presented in Figure 3.
The mean V_S values that we calculated for the four depth intervals (0-14 m, 14-31 m, 31-57 m, 57-178 m) in the array (Table 2) are compared to the V_S profile that has been previously derived on the basis of cross-hole and down-hole measurements down to 90 m and empirically assessed at larger depths (CORSEIS, 2002) (Figure 4). This previously suggested V_S profile, hereafter referred to as the "CORSEIS" V_S profile, has been recalculated at the depth intervals that we examined (blue continuous line in Figure 4) to make the comparison between our findings and pre-existing information more straightforward. Interferometry inferred V_S values are in very good agreement with the "CORSEIS" velocity profile at the resolution level that the vertical array sensors spacing imposes. The largest discrepancy occurs around 20 m, where our sampling interval smooths out the abrupt velocity change

detected by the geophysical measurements and at 31-57 m where interferometry inferred V_S is smaller by circa 25% the value of the "CORSEIS" model.

It should be mentioned that derived V_S values were checked against several measures such as the epicentral distance and magnitude of the studied events and the angle of incidence of the incoming waves and we found no correlations.

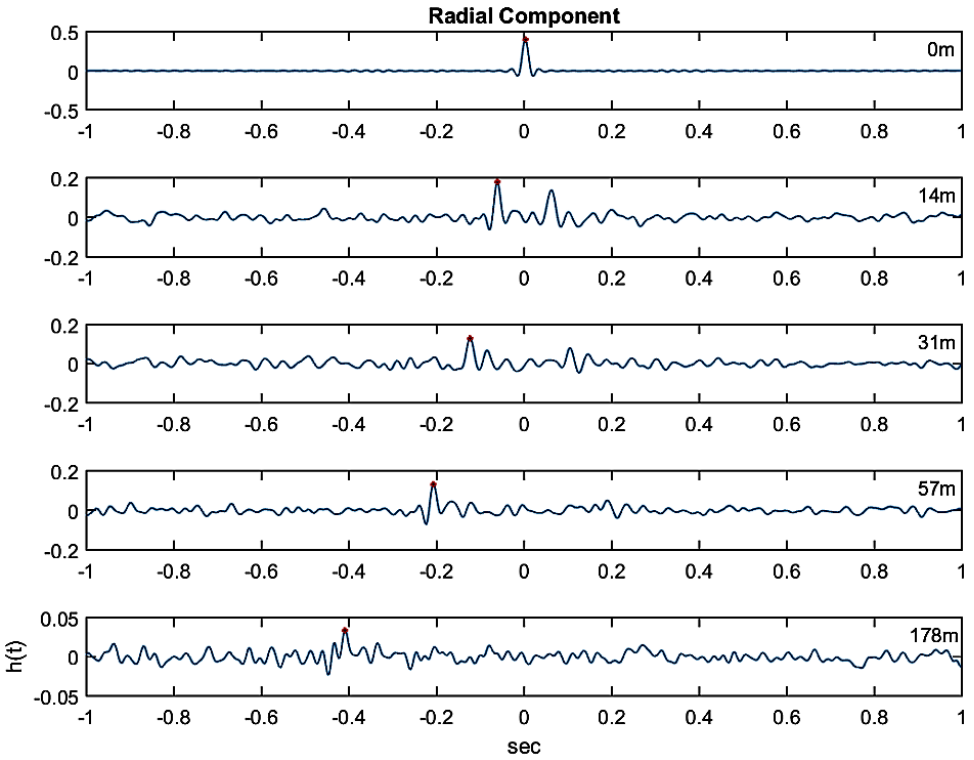

a)

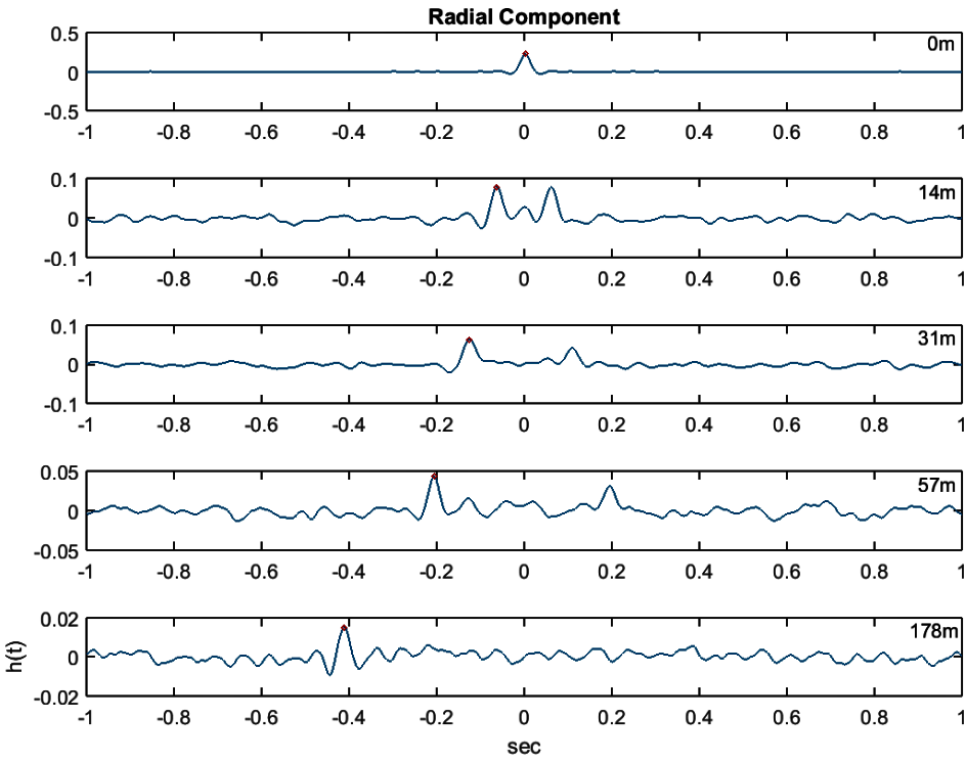

b)

Figure 3. Representative output of the seismic interferometry by deconvolution method at the CORSSA site: a) 21 January 2012, M_L3.1, R = 23 km earthquake and b) 15 March 2012, M_L4.4, R = 83 km earthquake. Interferograms at each subplot from top to bottom correspond to the deconvolution of waves at 0, 14, 31, 57 and

178 m deep sensors from the signal recorded at the ground surface (0 m). Results are those of the radial component. Red dots mark the time points used to compute the shear wave velocities at different depth intervals.

Table 1. Mean V_S values inferred from interferometry for the CORRSA site. Depth intervals are defined by the downhole sensors' installation depths.

Depth Interval (m)	***Vs*** (m/sec)
0-14	220
14-31	299
31-57	331
57-178	612

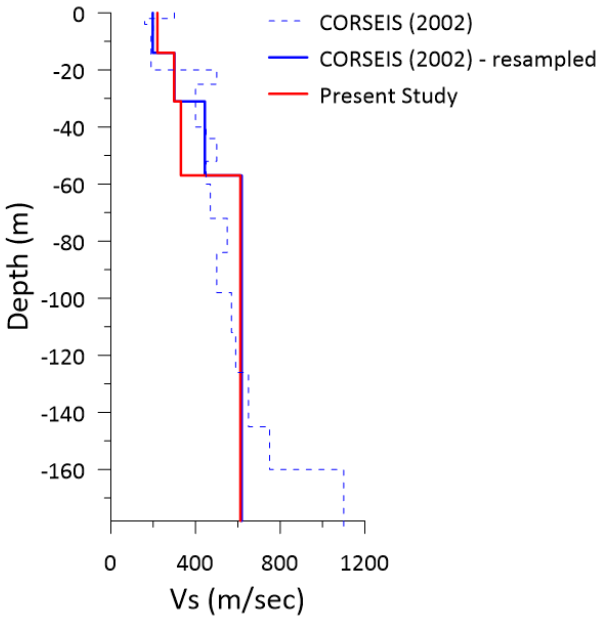

Figure 4. Comparison of interferometry inferred V_S profile at CORSSA with the profile proposed in the frame of the CORSEIS project (2002). Dashed line corresponds to the "CORSEIS" profile, continuous blue shows mean values of the "CORSEIS" profile at the depth intervals of the vertical array and red continuous line corresponds to the herein calculated velocities.

3. SHEAR-WAVE VELOCITY VARIATION

3.1 Seasonal Variation

The shear wave velocity, V_S, of a soil formation is influenced by its water content and, thus, by factors controlling it, such as the clay amount and the precipitation (e.g. Paoletti, 2012). Sens-Schönfelder and Wegler (2006) detected seasonal variations of seismic velocities, after applying passive image interferometry to continuous ground velocity data at Merapi volcano, Indonesia. They explained their observations by suggesting a simple hydrological model of the ground water level. More recently, Nakata and Snieder (2012) verified some negative correlation between seismic interferometry inferred V_S and precipitation after the analysis of a large number of accelerometric records at KiK-net stations in southern Japan.

To investigate possible seasonal variations in our V_S estimates at CORSSA site, we calculated the mean V_S per month (stacked over multiple years) and compared it to corresponding numbers for rainfall height at the nearby meteorological station of Aigio (Triantou, 2011). Rainfall in the study area is practically the only form of precipitation. The comparison between the two quantities is presented in Figure 5. In accordance with previous studies, we detect a negative correlation between V_S and precipitation. This relation is observable at 0-14 m and even at 14-31 m depth, while it disappears at deeper intervals, e.g.

the 31-57 m (Figure 5). This means that V_S at shallow depths decreases during the wet period, which for the Aigio area corresponds to the season October-April. Such a decrease is, of course, expected in theory, but herein we prove once more that it is traceable after the processing of actual ground motion recordings. The maximum variation at the top layer appears to be of the order of 6-7% with respect to the lowest mean value and drops to 3-4% at 14-31 m. These percentages, however, should be considered as the lower bound of the variation as the effect has been smoothed out due to the examination of monthly mean values. Sharp changes at shallow V_S values are expected when heavy rainfall follows an elongated dry period.

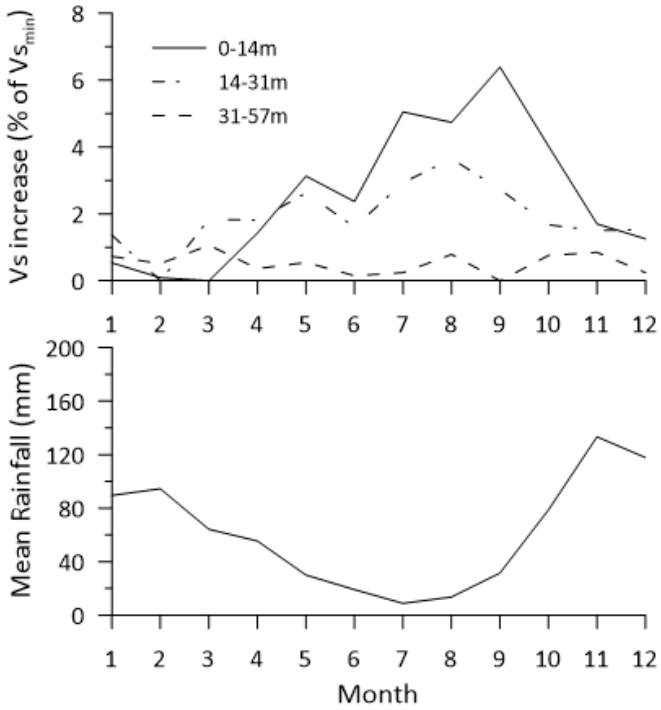

Figure 5. Variations of monthly mean shear-wave velocity, V_S, at different depth intervals, estimated as increase with respect to the minimum mean velocity throughout the year (top) and monthly variation of the mean rainfall (bottom).

3.2 Azimuthal Variation

Based on dipole sonic data in a close-by to CORSSA deep borehole (AIG10, e.g., Cornet et al., 2004), which cuts through the Aigio fault at 753-773 m depth, Prioul et al. (2004) revealed characteristics of azimuthal anisotropy of shear-wave velocity in certain parts of the well and homogeneous isotropic medium behavior in others. In areas where anisotropy was clear, its amplitude was found to be of the order of 9-25%, i.e., moderate-to-large and with the fast-shear azimuth at 105°. Prioul et al. (2004) suggested this anisotropy to be related to intrinsic characteristics, e.g., fractures and bedding oriented in a consistent manner with the regional maximum horizontal stress.

To investigate indication for similar or additional anisotropy within the shallow sedimentary formations, we rotated all pairs of horizontal recordings in our dataset from 0-360° with a 5° step and estimated V_S from interferometry. Then, for each rotation angle we used all available V_S values (from different events) to compute a mean V_S ($V_{Sazmean}$). We resulted in 72 mean V_S values corresponding to the 72 examined azimuths. We then derived the global mean (V_{Sgmean}) from the 72 $V_{Sazmean}$ values. Anisotropy was, finally, determined from the relation:

$$Anisotropy = \frac{V_{Sazmean} - V_{Sgmean}}{V_{Sgmean}} \times 100 \quad (3)$$

Results for the 0-178 m interval, as well as for sub-intervals, are presented in Figure 6.

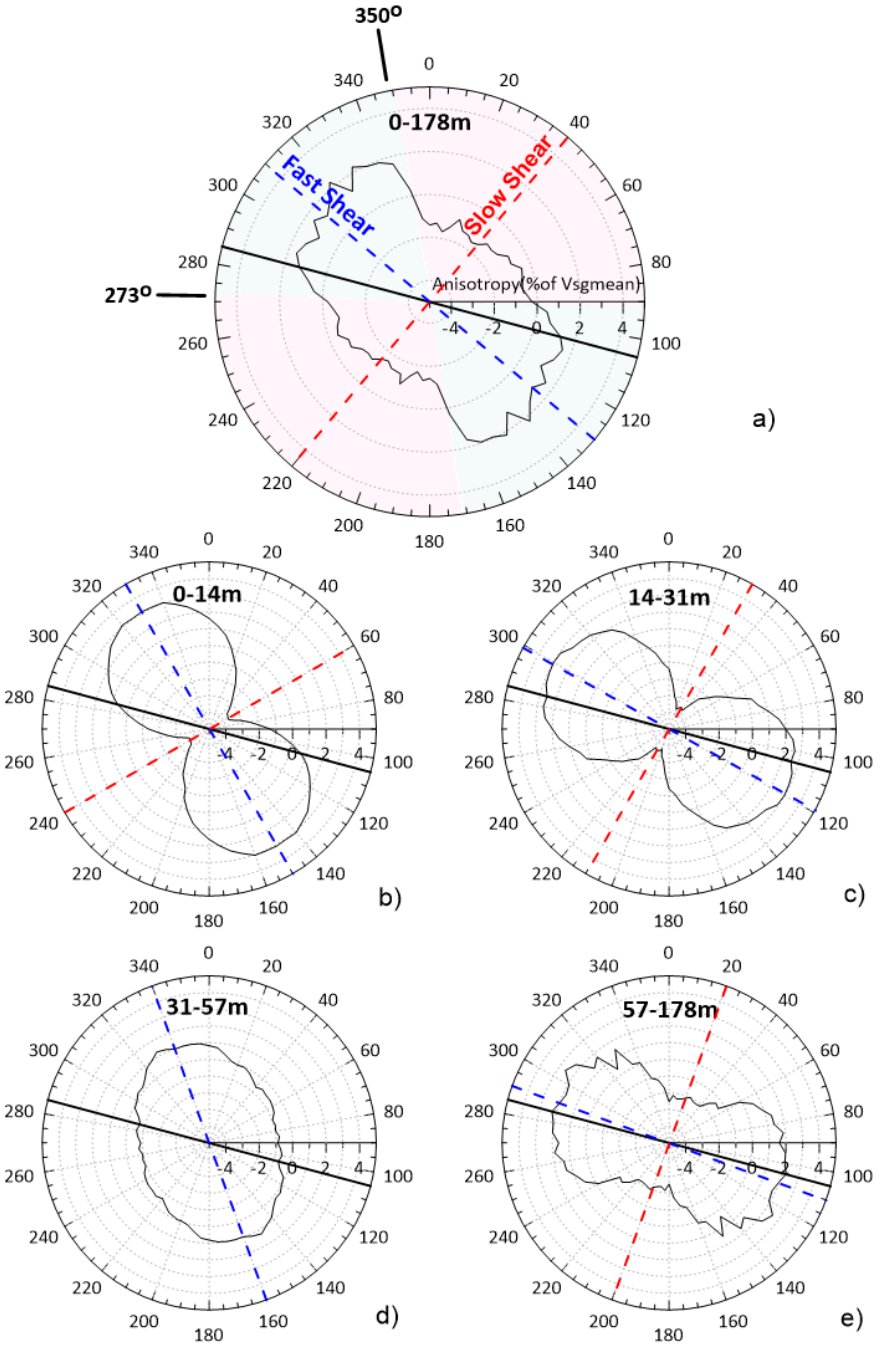

Figure 6. Polar plots of anisotropy values estimated from relation (3) described in the text. Value "0" in the radius axis of each plot corresponds to the mean V_S value derived over many processed events and 72 rotation angles. Black thick line marks the fast-shear orientation suggested by Prioul et al. (2004) well beneath the sediments, blue and red dashed lines correspond to shear fast- and slow-shear directions defined herein, respectively. a) Anisotropy inferred for the entire soil column (0-178 m). Areas of fast and slow shear-wave velocity are marked by light blue and pink colors. Transition zones are centered at 273° and 350°. Anisotropy values are shown separately for the b) 0-14 m, c) 14-31 m, d) 31-57 m and e) 57-178 m depth intervals.

Figure 6a, i.e, the polar plot of the anisotropy values computed for the entire soil column (0-178 m) suggest the existence of wide fast-shear (light blue) and slow-shear (pink) sectors, well defined by narrow zones of fast transition from one sector to the other. This is particularly true for the 350°-170° direction, where V_S takes either maximum or minimum values within a zone of 5°. In the almost conjugate direction, which coincides with the strike of Aigio Fault, the transition from lowest to highest

V_S takes place within 173° ± 15°. The center of the defined fast-shear zone appears to be rotated by 25° northward with respect to the fast-shear direction of Prioul et al. (2004). Nevertheless, when the deepest sensors pair is examined (Figure 6e), the two directions practically coincide. Taking into account the patterns in Figures 6b-d, as well, it seems that the direction of anisotropy changes within different layers. A close to N-S fast-shear direction is inferred at shallower depths and its combination with the almost E-W fast-shear at depth provides the hybrid pattern of Figure 6a. Minimum V_S appears in all cases in the fault-parallel direction. Overall, azimuthal variance of V_S appears to be of the order of ± 4% of the V_{Sgmean}. A similar amplitude in anisotropy has been derived through seismic interferometry by deconvolution on the accelerometric records of the Garner Valley, California, vertical array (Chandra et al. 2015).

3.3 Evidence for Shear-Wave Velocity Reduction Due to Nonlinear Response of the Soil

Records of the 2008 SW Achaia earthquake (08 June 2008, M_L6.4, R = 58 km), which are the strongest in terms of PGA in the studied dataset (e.g., PGA > 90 cm/sec^2 at the EW component of ground motion at the wellhead) were investigated for evidence of nonlinear behavior of the soil during strong shaking. One of the expressions of the nonlinear behavior of the soil is a reduction in the shear-wave velocity. It is, thus, one of the factors that could contribute to shear-wave velocity variation at a site and under this prism, it is being investigated in this section.

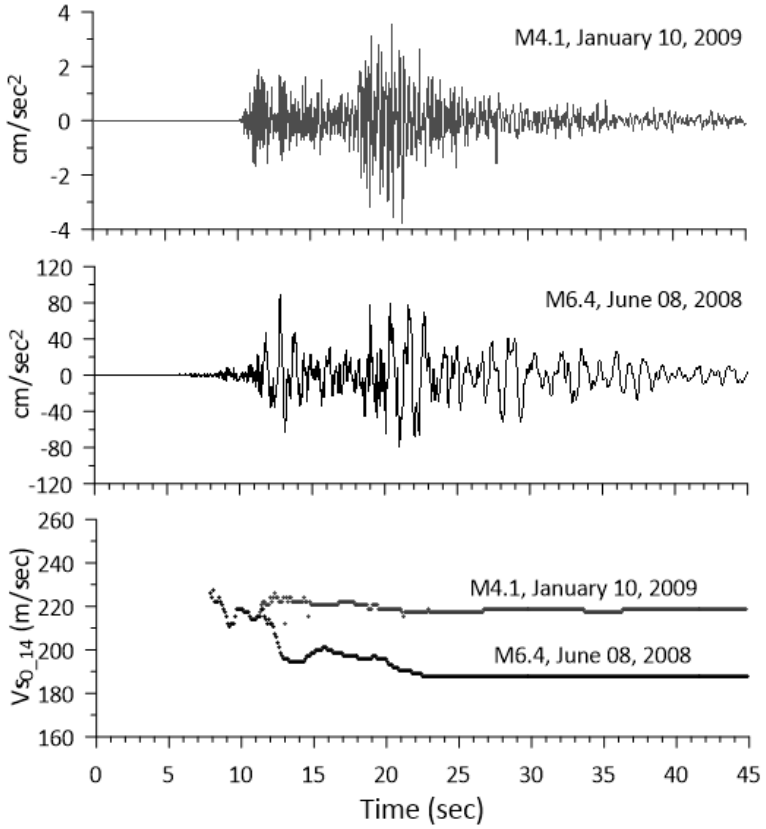

Figure 7. Acceleration records in the radial (epicenter-to-CORSSA) direction of two events of similar focal location and significantly different magnitude (top: M_L4.1 of January 10, 2009; middle: M_L6.4 of June 08, 2008). Bottom plot shows the interferometry-inferred V_S values within the top 14 meters of the CORSSA soil column for time windows that initiate at the beginning of the plotted traces, t_P and whose duration gradually increases from 1 to 44 sec, i.e. each small symbol in the bottom plot corresponds to a different V_S estimation. Plotted V_S values fulfill the quality criteria set in the present work (section 3).

In Figure 7, we present plots of the radial (i.e., epicenter-to-site) horizontal component of ground acceleration at the CORSSA surface station, as caused by two earthquakes of very close foci but quite different magnitude: the 2008 SW Achaia earthquake (M_L6.4; R = 58 km; Backazimuth, Baz = 238°) and a close by to the previous earthquake which occurred on the 10th of January, 2009 (M_L4.1;

R = 54 km; Baz = 241°). In the same Figure, we also plot the interferometry-inferred V_S values within the top 14 meters of the CORSSA soil column for time windows that initiate at the beginning of the plotted traces, t_P and whose duration gradually increases from 1 to 44 sec, i.e. each tiny symbol in the bottom plot corresponds to a different V_S estimation. All plotted V_S values fulfill the quality criteria set in the present work (see section 3). The temporal V_S variation associated to the M_L4.1 earthquake is representative of most similar computations performed in the frame of the present work, i.e., the vast majority of the examined events resulted in only slight (practically insignificant) variation of the measured V_S after the arrival of the shear-waves. The analysis of the 2008 SW Achaia earthquake record, on the other hand, provided an indisputably different picture with a very sharp decrease in measured velocity on the arrival of the first strong, large-period pulse. Other, although less abrupt changes in V_S are observed after this profound "step" in extracted values. Figure 7 provides evidence that the top soil formations at CORSSA may have behaved nonlinearly during the shaking caused by the 2008 SW Achaia earthquake and that this nonlinear behavior caused a considerable reduction in measured velocity. To quantify this effect in a statistically significant sense, more strong motion records are required.

5. CONCLUSIONS

Acceleration records of the CORSSA vertical array in the southern coast of the Gulf of Corinth have been used in an interferometry by deconvolution study, aiming at the computation of shear-wave velocity in the soil formations and the study of its variations. The derived V_S profile, with a resolution controlled by the geometry of the array (i.e., spacing between the array sensors), was found to be in very good agreement with independent information from geophysical measurements.

The investigation of the extracted V_S values with respect to their temporal distribution revealed a clear variation depending on the season and more specifically on the precipitation. It seems that rainwater entering the shallow soil formations alters their moisture content in a way that is traceable in ground acceleration records. The seasonal variation of V_S at the CORSSA site diminishes with depth and becomes practically untraceable deeper than circa 30 m. At depths of 0-14 m, however, the variation is of the order of 6-7%, and may be significantly larger closer to the ground surface where soil experiences the largest moisture content alteration after heavy precipitation episodes.

A directional dependence of V_S was also inferred both at the ground surface and at the various levels of the downhole sensors. Fast-shear direction in the deepest examined interval (57-178 m) was found close to 100°-280°, in excellent agreement with previous estimates based on dipole sonic data on a nearby to CORSSA deep borehole. Another direction quite close to N-S appears at shallower depths and as its effect is superimposed on the effect of the deeper anisotropy, the result is a hybrid pattern at the ground surface with high V_S in the NW and SE quartiles of the polar plots and low V_S in the NE and SW quartiles. Transition zones from highest to lowest V_S are centered at 173° and 350° and are quite narrow, especially the latter one. The correlation of these directions to existing fault and fracture directions in the study area and to other mechanisms such as preferably oriented deposition process of the sediments requires further investigation.

Although aforementioned variations of V_S appear to be relatively small at the mean values level (4-7%), large variations may be observed under special conditions. An example was provided through the study by interferometry of the acceleration records of the M_w6.4 SW Achaia earthquake (08 June 2008). Although PGA at CORSSA surface station was slightly above 90 cm/sec^2, herein analysis inferred a significant reduction in measured velocity, which is most probably related to nonlinear behavior of the shallow soil formations.

Overall, the results of the interferometry by deconvolution analysis presented highlights once more the potential of this method. Besides its effectiveness in the determination of the mean shear-wave velocity, the method succeeded in tracing small changes of the measured quantity. Further studies are required to quantify these phenomena in a more general context and to understand the physics behind them. It is also of interest to study the combined effect of such variations, which may be additive or destructive depending on the special conditions (e.g., increased soil moisture and nonlinear behavior of the soil at the same time) during the occurrence of an earthquake event.

6. ACKNOWLEDGMENTS

This work was performed in the frame of the Sinaps@ project that receives funding managed by the French National Research Agency under the program "Future Investments" (Sinaps@ reference: ANR-11-RSNR-0022). Sinaps@ is coordinated by the "SEISM Institute" (http://www.institut-seism.fr/en/). We thank Professors D. Raptakis of Aristotle University of Thessaloniki and P.-Y. Bard of Université Grenoble Alpes for intrinsic discussions on the topic of this work.

7. REFERENCES

Abrahamson NA (2007). Program on technology innovation: Effects of Spatial Incoherence on Seismic Ground Motions, *EPRI, Final Report*, Palo Alto, CA, 1015110, pp. 98.

Apostolidis PI, Raptakis DG, Pandi KK, Manakou MV, Pitilakis KD (2006). Definition of subsoil structure and preliminary ground response in Aigion city (Greece) using microtremor and earthquakes, *Soil Dyn. and Earthq. Eng.*, 26: 922-940.

Armijio, R, Meyer B, King GCP, Rigo A, Papanastassiou D (1996). Quaternary evolution of the Corinth rift and its implications for the late Cenozoic evolution of the Aegean, *Geophys. J. Int.*, 126: 11-53.

Bonilla LF, Guéguen Ph, Lopez-Caballero F, Mercerat ED, Gélis C (2017). Prediction of non-linear site response using downhole array data and numerical modeling: The Belleplaine (Guadeloupe) case study, *Physics and Chemistry of the Earth*, 98: 107 – 118.

Boore DM, Bommer JJ (2005). Processing of strong-motion accelerograms: needs, options and consequences, *Bull. Seism. Soc. Am.*, 25: 93 - 115.

Chandra J, Guéguen Ph, Steidl JH, Bonilla LF (2015). In Situ Assessment of the *G-γ* Curve for Characterizing the Nonlinear Response of Soil: Application to the Garner Valley Downhole Array and the Wildlife Liquefaction Array, *Bull. Seism. Soc. Am.*, 105(2A): 993-1010.

Cornet FH, Doan ML, Moretti I, Borm G (2004). Drilling through the active Aigion Fault: the AIG10 well observatory, *Comptes Rendus Geoscience*, 336(4-5): 395-406.

CORSEIS (2002). Project Final Report.

Gallovic F, Zahradnik J, Krizova D, Plicka V, Sokos E, Serpetsidaki A, Tselentis G-A (2009). From earthquake cetroid to spatial-temporal rupture evolution: Mw6.3 Movri mountain earthquake, June 8, 2008, Greece, *Geophysical Research Letters*, 36, L21310, doi: 10.1029/2009GL040283.

Ganas A, Serpelloni E, Drakatos G, Kolligri M, Adamis I, Tsimi Ch, Batsi E (2009). The Mw 6.4 SW-Achaia (Western Greece) earthquake of 8 June 2008: Seismological field, GPS ob-servations, and stress modeling, *Journal of Earthquake Engineering*, 13(8): 1101-1124.

Guéguen Ph (2015). Predicting nonlinear site response using spectral acceleration V_S PGV/V_S30: A case history using the Volvi-Test site, *Pure Appl. Geophys.*, 173(6): 2047-2063.

Jolivet L, Labrousse L, Agard P, Lacombe O, Bailly V, Lecomte E, Mouthereau F, Mehl C (2010). Rifting and shallow-dipping detachments, clues from the Corinth rift and the Aegean, *Tectonophysics*, 483: 287-304.

Kassaras I, Roumelioti Z, Ktenidou O-J, Pitilakis K, Voulgaris N, Makropoulos K (2016). Accelerometric data and web portal for the vertical Corinth Gulf Soft Soil Array (CORSSA), Bulletin of the Geological Society of Greece, Vol. L; *Proc. of the 14th Intern. Congress of the Geological Society of Greece*, 25-27 May, Thessaloniki, Greece.

Koukouvelas I (1998). The Egion fault earthquake-related and long-term deformation, Gulf of Corinth, Greece, *J. Geodyn.*, 26(2-4): 501-513.

Koukouvelas I, Doutsos T (1996). Implications of structural segmentation during earthquakes: The 1995 Egion earthquake, Gulf of Corinth, Greece, *J. Struct. Geol.*, 18(12): 1381-1388.

Mehta, K, Snieder R, Graizer V (2007). Downhole receiver function: a case study, *Bull. Seism. Soc. Am.*, 97(5): 1396-1403.

Nakata N, Snieder R (2011). Near surface weakening in Japan after the 2011 Tohoku-Oki earthquake, *Geophys.*

Res. Lett., 38: L17302.

Nakata N, Snieder R (2012). Estimating near-surface shear wave velocities in Japan by applying seismic interferometry to KiK-net data, *J. Geophys. Res.*, 117: B01308, 1-13.

Palyvos N, Pantosti D, De Martini PM, Lemeille F, Sorel D, Pavlopoulos K (2005). The Aigion-Neos Erineos coastal normal fault system (western Corinth Gulf Rift, Greece): Geomorphological signature, recent earthquake history, and evolution, *J.Geophys. Res.*, 110: B09302, 1-15.

Paoletti V (2012). Remarks on factors influencing shear wave velocities and their role in evaluating susceptibilities to earthquake-triggered slope instability: case study for the Campania area (Italy), *Nat. Hazards Earth Syst. Sci.*, 12: 2147-2158.

Prioul R, Plona Th, Kane M, Sinha B, Kaufman P, Signer C (2004). Azimuthal anisotropy using shear dipole sonic: insights from the AIG 10 well, Corinth Rift Laboratory, *Comptes Rendus Geosciences*, 336: 477-485.

Reilinger R, McClusky S, Paradissis D, Ergintav S, Vernant P (2010). Geodetic constraints on the tectonic evolution of the Aegean region and strain accumulation along the Hellenic subduction zone, *Tectonophysics*, 488: 22-30.

Sawazaki K, Sato H, Nakahara H, Nishimura T (2009). Time-lapse changes of seismic velocity in the shallow ground caused by strong motion shock of the 2000 Western-Totori earthquake, as revealed from coda deconvolution analysis, *Bull. Seism. Soc. Am.*, 99(1): 352-366.

Sens-Schönfedler C, Wegler U (2006). Passive image interferometry and seasonal variations of seismic velocities at Merapi volcano, Indonesia, *Geophys. Res. Lett.*, 33, L21302, doi: 10.1029/2006GL027797.

Triantou AG (2011). Hydrogeological study of the Aigio area, *Research Thesis*, Department of Geology, University of Patras, pp. 71 (in Greek).